Kinematic Correction for Energy Resolution Improvement Using a Position Sensitive Detector

Ossama A. Abouzeid
Department of Physics
University of Manitoba
Winnipeg, Man., Canada.

A thesis submitted to the Faculty of Graduate Studies of the University of Manitoba in partial fulfillment of the requirements for the Degree of Master of Science

February 1977

"KINEMATIC CORRECTION FOR ENERGY RESOLUTION IMPROVEMENT USING A POSITION SENSITIVE DETECTOR"

by

OSSAMA A. ABOUZEID

A dissertation submitted to the Faculty of Graduate Studies of the University of Manitoba in partial fulfillment of the requirements of the degree of

MASTER OF SCIENCE

TO MY PARENTS

ACKNOWLEDGMENTS

I would like to express my gratitude to my advisor Dr. W.R. Falk for his assistance and quidance during this work. I would like also to thank Dr. L.Ph. Roesch and Dr. P. Debenham for their help.

In addition I would like to thank the members of the electronic and mechanical shops.

Finally I would like to express my appreciation for the financial support given by Physics Department and Cyclotron Laboratory .

Abstract

A technique has been developed that improves the energy resolution in scattering experiments that use a highly divergent accelarator beam.

The technique is described in the main body of this thesis and involves shifting the usual beam waist (an upright phase space ellipse) at the target position to a point downstream from the target. The distance to which the waist should be moved depends on the scattering angle, target angle, and the beam properties.

The technique was tested by computer program and an improvement in the energy resolution by a factor of 4 - 8 was obtained. Experimental measurements on carbon and hydrogen targets were performed using a position sensitive detector. The results showed the technique to be effective. Angular resolution is improved as a consequence of energy resolution improvement.

The introductory chapter contains a summary of the details and the design consideration of the momentum analysis system of the high resolution beam line. An understanding of the entire system is mandatory for the experimental tests of the theory put forward in this thesis.

contents

List of tables

List of Figures

Introduction

The beam delivered by the momentum analysis system of the high resolution beam line of the University of Manitoba Cyclotron will result in an angular divergence of up to $\pm 2^{\circ}$ on the target. The kinematic energy resulting from this divergence is very serious for the lighter nuclei where the kinematic energy spread per degree is large. For heavier nuclei, where the kinematic energy spread may not be serious, this angular divergence may, however, be unacceptably large for measurement of an angular distribution.

This thesis describes a technique that improves remarkably the energy resolution in scattering experiments, and results in a corresponding improvement in the angular resolution of the experiment. The latter point is of importance in studying angular distributions that vary rapidly with angle, while utilizing the full beam acceptance. The technique involves shifting the usual beam waist at the target position to a point downstream from the target. A similar technique, known as dispersion matching[15], is well known and applied in magnetic spectrograph detector systems which are matched to the characteristics of the beam incident on target by appropriate shifting of the strengths of quadrupole singlets in the transport system to give a dipersion such that all

particles (for certain reaction) are brought to the same point in the focal plane of the spectrograph. The detector system used in this work is a more conventional one comprising a solid state position sensitive detector with a solid angle of up to 7 mstr, where the position information can be used to apply kinematic correction from the angular information.

The thesis is divided into 4 chapters and is comprised of two parts. The first is described in chapter 1 and represents a summary of the essential design considerations, beam behaviour, and the details of the momentum analysis system of the high resolution beam line. This work was done mainly by P. Debenham and W. Falk during the period 1970 1974[1]. Furthermore, the effect of the second-order aberrations on the quality of the image at the focal plane of the analysis system has been investigated.

The second part of this thesis then represents a description of the technique mentioned earlier to improve the energy resolution and it is described in the remaining 3 chapters.

Chapter 2 describes the theory and conditions that should be satisfied in order to improve the energy resolution. It also contains the theoretical calculations done to test the theory using a special computer program.

Chapter 3 contains the experimental procedure, electronics used, and description of the computer programs used with the position sensitive detector.

Chapter 4 describes all the experimental results obtained for the reactions $^{12}C(p, \ )^{9}B$, and $^{1}H(p,p)^{1}H$. Also it gives a comparison between the measured energy resolution improvement and the energy resolution improvement predicted by the theory.

CHAPTER 1

High Resolution Beam Analysis System

1.1 Introduction

The high resolution beam analysis system has been designed to accept as an input a beam of emittance as high as 15 mm.mrad (half width times half divergence) and provide at the targrt position a beam of intensity 1% of the intensity on slits s1 shown in fiq(1.1) , and a final intirinsic energy resolution $\frac{\Delta E}{E} = 5 \times 10^{-4}$ (1).

The system was built on the 15° right beam line.For economic reasons and space limitation the system was choosen to consist of two 90° single focusinq analyzinq magnets of 30 in. radius .The two maqnets bend in opposite directions to each other,so in this way the dispersions of the two magnets will add (3).
Technical data for the two analyzinq maqnets is qiven in Table(1.1). Fiq(1.2)shows a schematic diaqram for the maqnet pole piece .

1.2 System Layout

Fiq(1.3) shows the layout of the system . It should be noticed that the dimensions indicated are measured between the effective field boundaries (EFB) of maqnets and centre of slits.

1.3 Uniform Field Measurement

The average fields on the central orbit in both magnets were measured using Hall probe type BHT 910 .

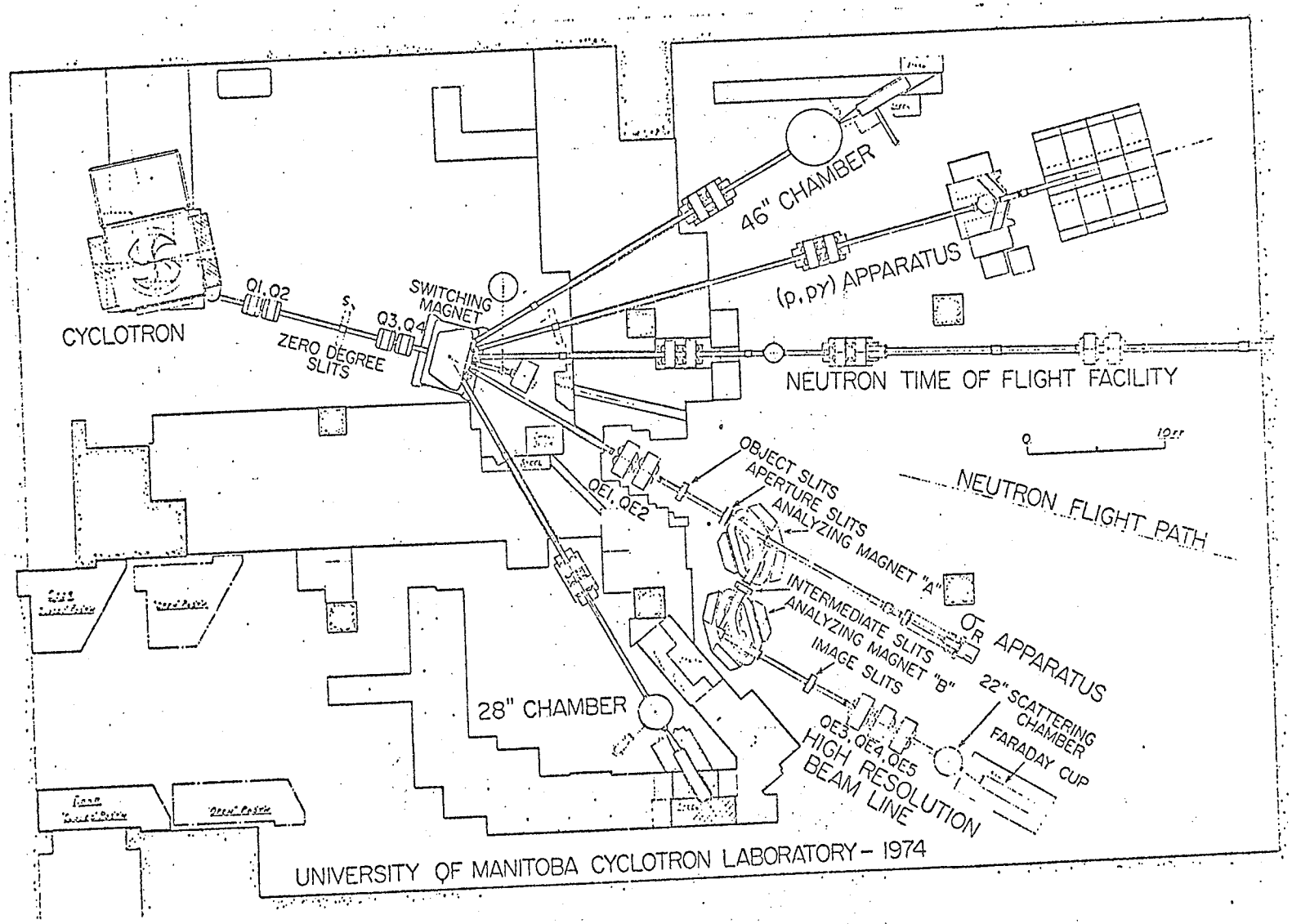
CYCLOTRON
Q1, Q2
ZERO DEGREE SLITS
Q3, Q4
SWITCHING MAGNET
46" CHAMBER
(p, pγ) APPARATUS
NEUTRON TIME OF FLIGHT FACILITY
NEUTRON FLIGHT PATH
OBJECT SLITS
APERTURE SLITS
ANALYZING MAGNET "A"
QE1, QE2
INTERMEDIATE SLITS
ANALYZING MAGNET "B"
IMAGE SLITS
QR APPARATUS
22" SCATTERING CHAMBER
FARADAY CUP
QE3, QE4, QE5
HIGH RESOLUTION BEAM LINE
28" CHAMBER
UNIVERSITY OF MANITOBA CYCLOTRON LABORATORY – 1974

Fig (1.1)

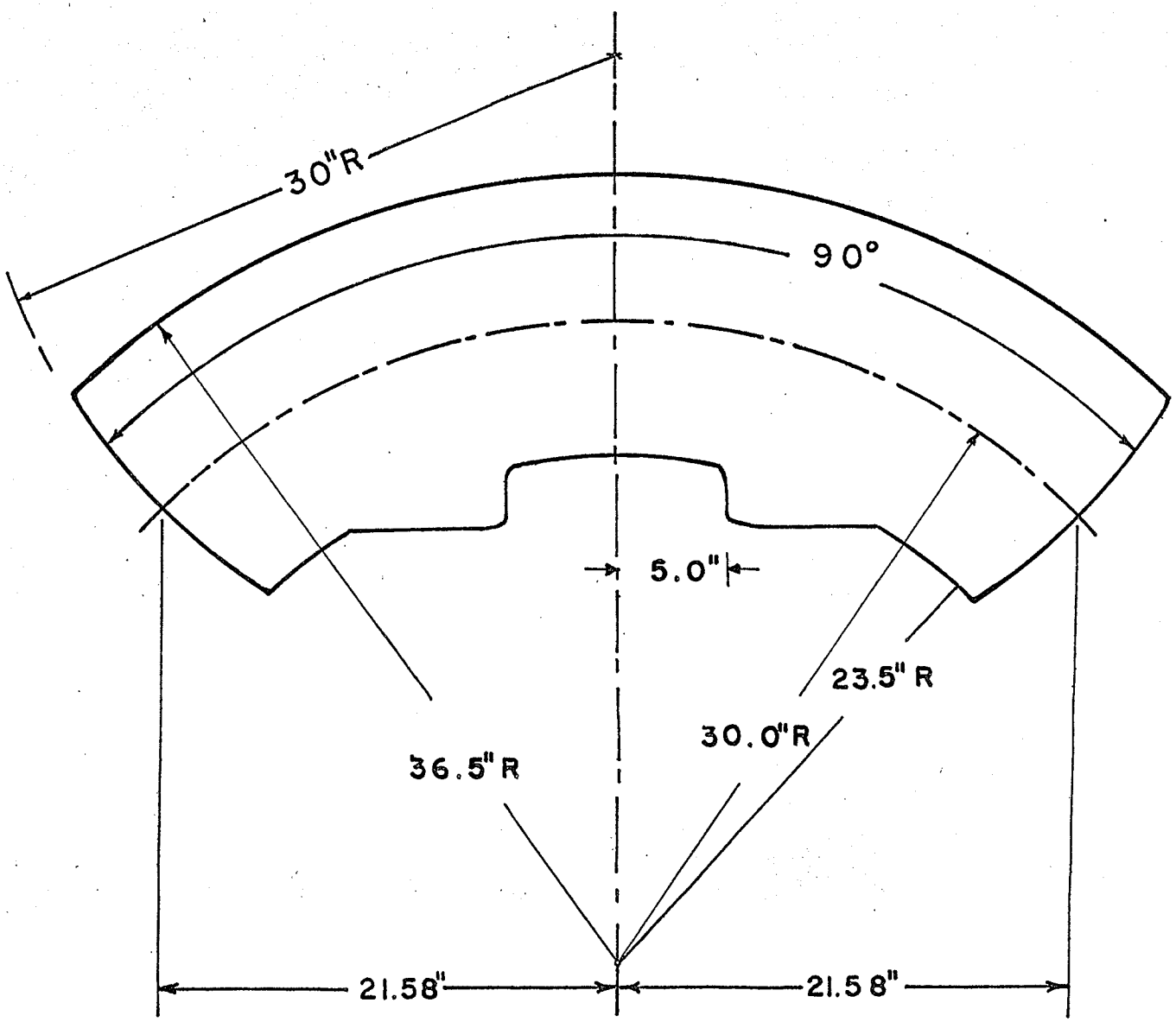

Fig (1.2) The Analyzing Magnet

TABLE (1.1)

ANALYZING MAGNET DATA

Bending radius	30 in.
Magnetic bending angle	90°
Air gap	1.75 in.
Pole width	13 in.
Max. field	14 KG
Entrance angle	0°
Exit angle	0°
Curvature of entrance angle	30 in.
Curvature of exit edge	30 in.
EFB (inside the pole root)	0.52 in.
Magnetic field index	0

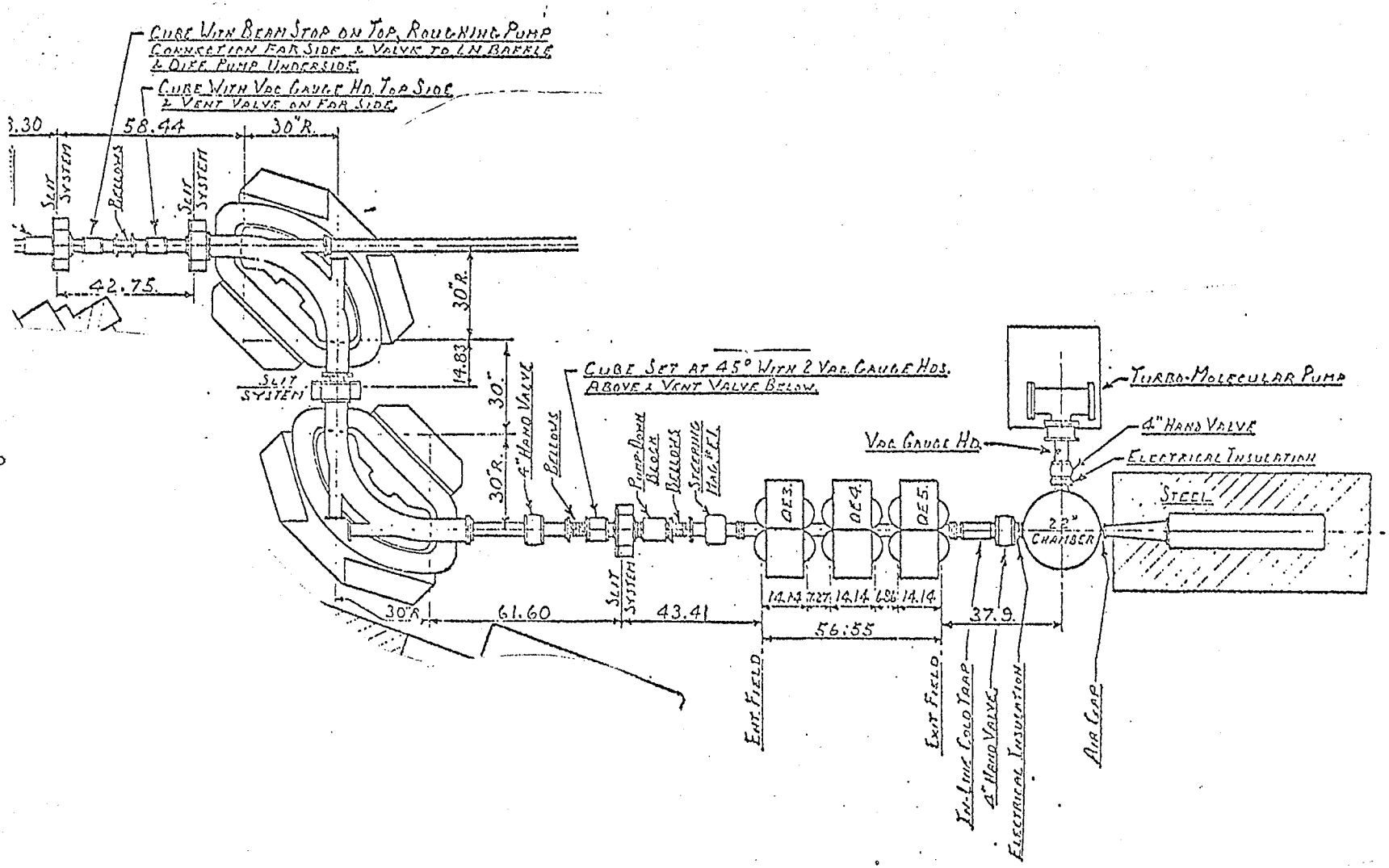

Fig (I.3) Momentum Analysis System Layout

The field non-reproducibility was found to be $\Delta B/B = \pm 5 \times 10^{-4}$. This was interpreted to be due to hysteresis. An investigation was made on the effect of this non-reproducibility on the quality of the image at the focal position, but it was found that it has a negligible effect.

The ratio between the average fields on the central orbits in both magnets was also measured . It was found that this ratio varies from 1.004 to 1.006 as the excitation varies from 9.5 KG to 12.5 KG. This required a proper adjustment of the trim coil current in order to maintain the same value of the field in both magnets.

The most intersting result of this mapping was that the field actually is not uniform(n=0) but it is slightly non-uniform. If we express the field in the form :

$$B(R) = B(R_0)\left[1 - n\left(\frac{R-R_0}{R_0}\right) + \beta\left(\frac{R-R_0}{R_0}\right)^2 + \gamma\left(\frac{R-R_0}{R_0}\right)^3 + \cdots\right]$$

where

$B(R_0)$ is the nominal field on the central ray (radius=R_0)

$B(R)$ is the field on the ray with bending radius = R

n, β, γ are the field indices.

It was found that the value of the field indices for both magnets are not the same. these values were :

1. For the first magnet : (the upsteam one)

   $n = -9.379 \times 10^{-3}$

   $\beta = -5.21 \times 10^{-2}$

   $\gamma = -.7253$

2. For the second magnet : (the downstream one)

$n = 2.7323 \times 10^{-3}$

$\beta = 1.05 \times 10^{-3}$

$\gamma = .2963$

This non-uniformity was found to have a negligible effect on both the quality and the position of the image.

1.4 Fringing Field Mapping

The actual bending radius increases steadily in the fringing field, so the real and the effective edge paths are separated by a small displacement which can be neglected in first order theory[3]. But for second-order calculations, this should be taken into consideration.

So, a mapping of the fringing field should be done carefully for both magnets. It was found that both magnets have similar fringing fields for both entrance and exit. Fig(1.4) shows the mapped median plane fringing field for the entrance of the first magnet (the upstream one) at an excitation of 11.5KG. The value of the tail was found to vary with the excitation from 1/4%B_o at excitation 9.5 KG to 1/2%B_o at excitation 13.5 KG, where B_o is the average field on the central orbit inside the magnet. This tail value implied the change of the object and the image distances from the ideal theoretical values to those appearing in Fig(1.3) in order to get an optimized image.

A theoretical fit for the measured fringing field was done, and it was found that the following Fermi function

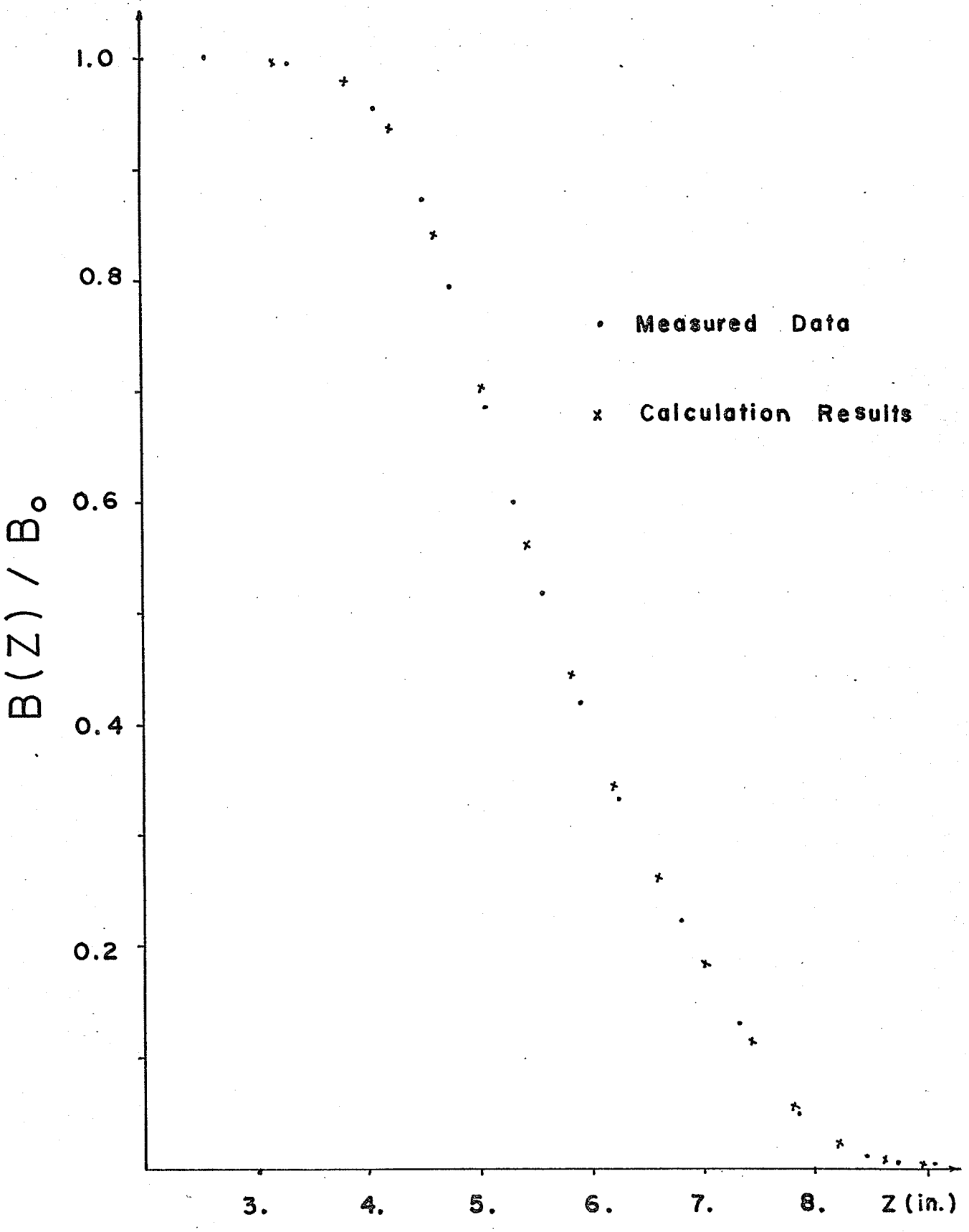
1.0
0.8
0.6
0.4
0.2
B(Z) / B₀
• Measured Data
x Calculation Results
3.
4.
5.
6.
7.
8.
Z (in.)

Fig (1·4)

gave an appropriate fit :

$$B(Z) = B_0 \Big/ 1 + e^{c_0 + c_1 S + c_2 S^2 + \cdots + c_5 S^5} \qquad (1.1)$$

where

B(Z) = The value of the field at distance Z measured from the pole root of the magnet.

B = Field on the central ray inside the magnet.

$S = Z - Z_{EFB} / G$

G = Air gap.

$c_0, c_1, c_2, c_3, c_4, c_5$ are constants.

The values of the constants $c_0, c_1, c_2, c_3, c_4, c_5$ which gave the best fit for both magnets were calculated to be as follows :

$c_0 = 0.135$

$c_1 = 2.0857$

$c_2 = -0.508$

$c_3 = 0.7223$

$c_4 = 0.0252$

$c_5 = -0.0128$

Fig (1.4) shows the fringing field shape as calculated using the above values.

1.5 Computer Programs

Several computer programs were used to study the magnetic analysis system and the beam behaviour through the system. So, it may be helpful to discuss these computer codes before we proceed any further.

1.5.1 Program TRANSPORT[4]

This is a first- and second-order matrix multiplication ccmputer program. At any specified position in the system an arbitrary charged particle is represented by a vector (single column matrix) as follows :

$$X = \begin{bmatrix} x \\ x' \\ y \\ y' \\ l \\ d \end{bmatrix} \qquad (1.2)$$

where

x = The horizontal displacement of the arbitrary ray with respect to the assumed central trajectory.

x' = The angle this ray makes in the horizontal plane with respect to the assumed central trajectory.

y = The vertical displacement of the ray with respect to the assumed central trajectory.

y' = The vertical angle of the ray with respect to the assumed central trajectory.

l = The path length difference between the ray and the central trajectory.

d = The fractional momentum deviation of the ray from the assumed central trajectory.

Any element in the beam line is represented to the first-order by a square matrix R which describes the

action of this element on the particles coordinates. Thus the passage of a charged particle through the system may be represented by :

$$X(1) = R\ X(0)$$

where

$X(1)$ = The final coordinates of the particle under consideration.

$X(0)$ = The initial coordinates of the same particle.

If the particle has to traverse n elements so the matrix R will be the product of the individual matrices of the system elements :

$$R = R(n).R(n-1). \ldots .R(1)$$

The program calculates this cumulative transfer matrix and prints it out where desired.

Furthermore, the program calculates the second-order transfer matrix by adding another term to the above formalism. The components of the final vector in terms of the original , are now given by :

$$X_i\ (1) = \sum_j R_{ij}\ X_j\ (0) + \sum_{jk} T_{ijk}\ X_j\ (0)\ X_k\ (0) \qquad (1.3)$$

where R_{ij} and T_{ijk} are the elements of the first- and second-order transfer matrices, respectively. The suffixes i,j,k runs from 1 to 6 where x_1, x_2, x_3, x_4, x_5 ,and x_6 stands for x, x', y, y', l , and d respectively. The construction of the first- and secod-order transformation matrices is gives in appedix I.

Provision is made in this program to vary some

physical parameters of the elements comprising the system and to impose various constraints on the beam design. For example, varying the field strength values in a quadrupole triplet in order to get a waist at certain position.

1.5.2 Program RAYTRACE[5]

This Fortran program integrates the Lorentz equations of motion for a charged particle moving through an arbitrary magnetic field. Analytic expressions for the field (fringing or central) in the median plane is used as determined from the experimental data and/or mathematical models. A Taylor's expansion is used to determine the components of the field off the median plane (up to second-order terms). Using the expressions for the field the program is capable of tracing rays with arbitrary initial conditions through the system.

Besides, the program has the option of calculating the second-order transfer matrix and investigating higher order effects (third-order).

1.5.3 Program OPTIK[6]

This computer code calculates first-order transfer matrix based on the same theory discussed above in TRANSPORT. Moreover, the program investigates the second-order chromatic aberration effect.

1.6 Beam Behaviour

Rays were traced through the analysis system to study beam behaviour in both vertical and horizontal planes. The final coordinates of each ray at different points along the system were calculated using the computer code OPTIK described in section 1.5.3 .

1.6.1 The vertical behaviour

Fig(1.5) shows the behaviour of 42 Mev proton trajectories in the vertical plane (YZ). Starting with a vertically converging beam at slits S shown in Fig(1.1), a vertical waist can be formed between the quadrupole Q4 and the switching magnet. The initial values of the beam coordinates at the slits S were choosen such that they reflecl t the actual emittance measured there. Quadrupole doublet QE1,QE2 forms a large vertical waist half way between magnets. In this way the vertical beam envelope is approximately parallel and passes through the analyzing magnets gaps.

1.6.2 The horizontal behaviour

The horizontal behaviour of the beam (XZ-plane) through the system is shown in Fig(1.6). The quadrupole doublet QE1,QE2 shown in Fig(1.1) produces a horizontal waist of width 1mm and a negligible dispersion at the object slits. This will serve as an object for the first analyzing magnet, which forms a dispersed image half way between the two magnets. The second magnet will form a

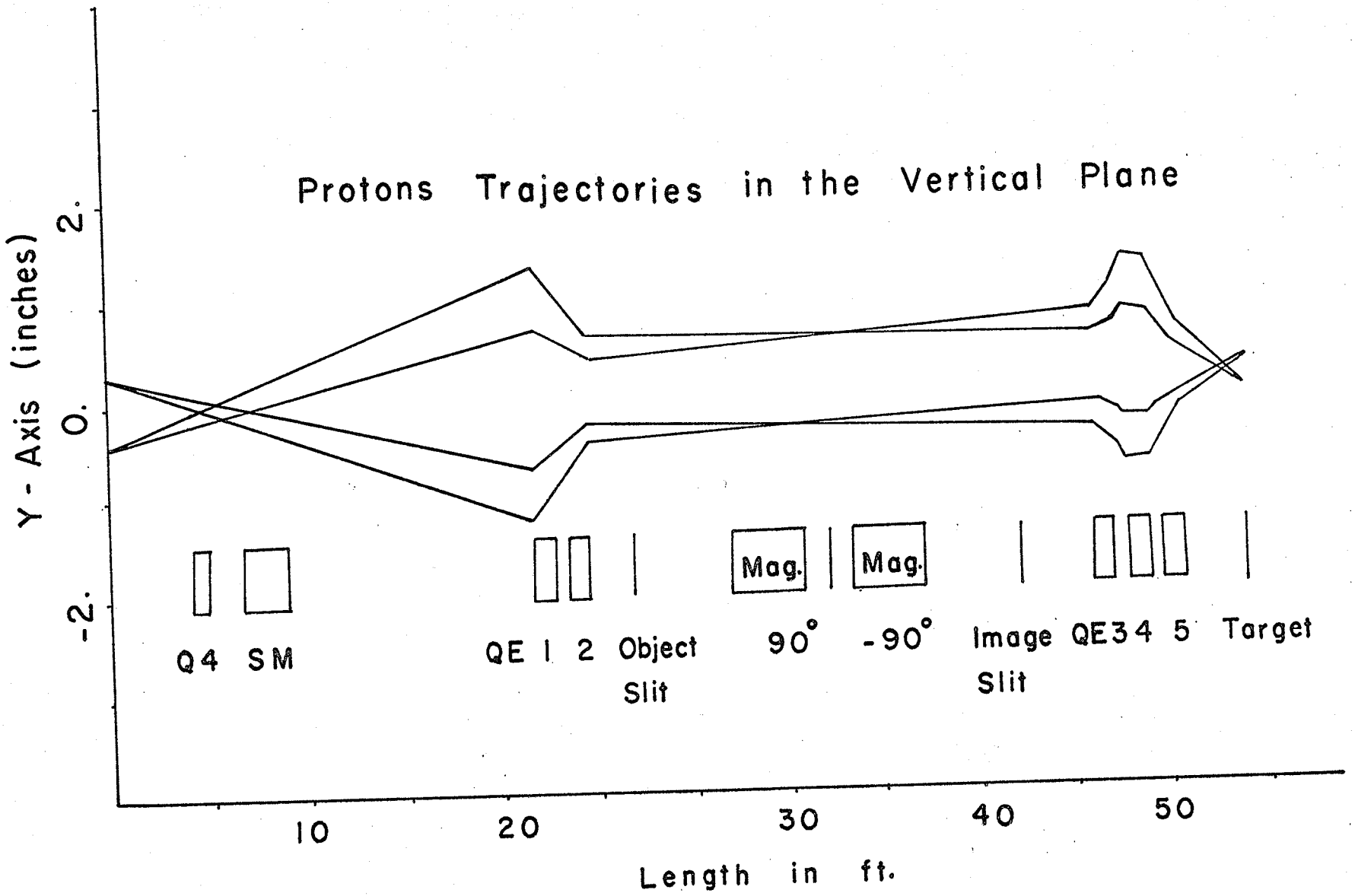
Protons Trajectories in the Vertical Plane
Y - Axis (inches)
2.
0.
-2.
Mag.
Mag.
Q4
SM
QE 1 2
Object Slit
90°
-90°
Image Slit
QE3 4 5
Target
10
20
30
40
50
Length in ft.

Fig (1.5)

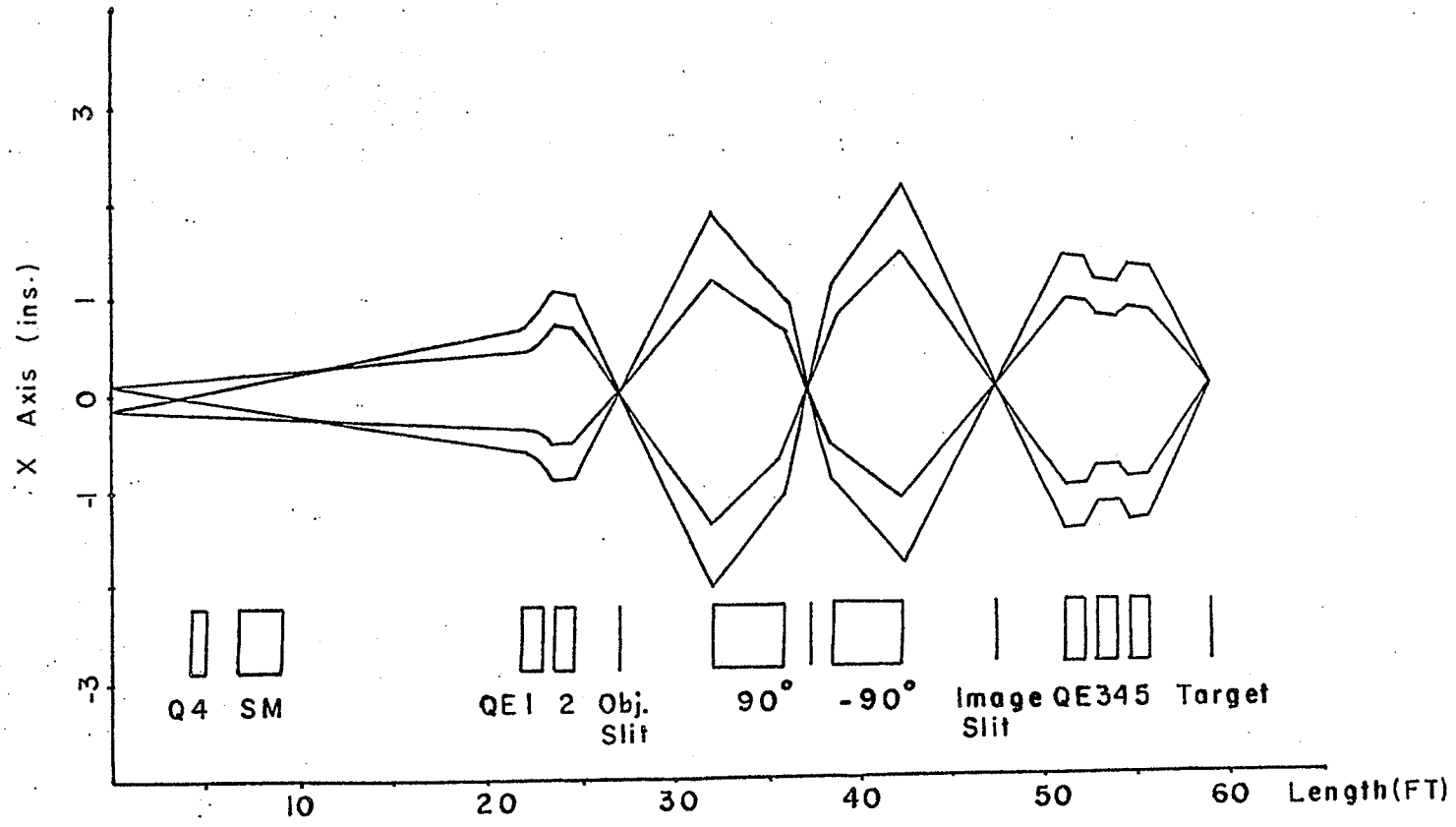

Fig (I.6) Protons Trjectories in the Horizontal Plane